Accepted Manuscript

Identification and functional characterization of a *MAX2* ortholog from switchgrass (*Panicum virgatum* L.)

Tingting Cheng, Donghua Wang, Yongfeng Wang, Shumeng Zhang, Chao Zhang, Shudong Liu, Yajun Xi, Fengli Sun

PII: S0981-9428(18)30216-X

DOI: 10.1016/j.plaphy.2018.05.016

Reference: PLAPHY 5263

To appear in: *Plant Physiology and Biochemistry*

Received Date: 29 January 2018

Revised Date: 9 May 2018

Accepted Date: 9 May 2018

Please cite this article as: T. Cheng, D. Wang, Y. Wang, S. Zhang, C. Zhang, S. Liu, Y. Xi, F. Sun, Identification and functional characterization of a *MAX2* ortholog from switchgrass (*Panicum virgatum* L.), *Plant Physiology et Biochemistry* (2018), doi: 10.1016/j.plaphy.2018.05.016.

Identification and functional characterization of a *MAX2* ortholog from switchgrass (*Panicum virgatum* L.)

Tingting Cheng[1, 2], Donghua Wang[1, 2], Yongfeng Wang[1, 2], Shumeng Zhang[1, 2], Chao Zhang[1, 2], Shudong Liu[1, 2], Yajun Xi[1, 2], Fengli Sun[1, 2*]

1 College of Agronomy, Northwest A&F University, Yangling, Shaanxi 712100, China;

2 State Key Laboratory of Crop Stress Biology for Arid Areas, Yangling, Shaanxi 712100, China;

[*]Corresponding authors: sunof1981@126.com

Abstract

Switchgrass (*Panicum virgatum* L.) is a sustainable cellulosic energy crop with high biomass yield on marginal soils. Tillering, an important agronomic characteristic related to biomass production in gramineous plants, is regulated by complex interacting factors, such as plant hormones. Strigolactones (SLs) comprise a novel class of plant hormones that inhibit shoot branching. The *MORE AXILLARY GROWTH2 (MAX2*)/*DWARF 3 (D3*)/*RAMOSUS (RMS4*) genes encode proteins involved in the SL signaling pathway in various plants. The switchgrass tetraploid genome likely contains two high-similarity *MAX2* homologues, one of which is 6 bp longer than the other. The longest is named *PvMAX2* and is the ortholog of *MAX2* in Arabidopsis, *D3* in rice, and *RMS4* in petunia. *PvMAX2* is expressed ubiquitously in switchgrass tissues, with higher expression levels observed in the stem and shoot. *PvMAX2* gene expression is upregulated by GR24, a synthetic SL analog. Ectopic expression of *PvMAX2* in the Arabidopsis *max2* mutant rescued the dwarf and bushy phenotypes and small leaf size in the mutant, suggesting that functions of *AtMAX2* in Arabidopsis are conserved in *PvMAX2*. Ectopic *PvMAX2* expression also restored the wild-type primary root and hypocotyl length phenotypes and restored the response to GR24. These results indicate that *PvMAX2* may play an important role in switchgrass tillering through the SL pathway.

Key words: Switchgrass, *PvMAX2*, Strigolactones, root, tillering

Abbreviations: SL, strigolactone; WT, wild type; MS, Murashige and Skoog; IAA, indole-3-acetic acid

1. Introduction

Switchgrass (*Panicum virgatum* L.), a native grass of North American prairies, is a perennial C4 plant that belongs to the genus *Panicum* L. (Poaceae) [1]. It is commonly used for soil and water conservation owing to its suitability to marginal land and strong adaptability. It has also been studied extensively as a model energy crop [2-5]. Tillering, a special form of branching in gramineous plants, is a primary agronomic characteristic responsible for biomass production [6]. Tillering is influenced not only by most environmental factors, such as temperature, soil nutrition, and cultivation measures, but also by biological factors, including hormones, and genetic factors [7-9].

Strigolactones (SLs), which are novel plant hormones, are terpenoid compounds that play an important role in suppressing shoot branching [10-13]. Recently, a series of branching mutants *MORE AXILLARY GROWTH* (*MAX*) in *Arabidopsis thaliana*, *DWARF* (*D*) in *Oryza sativa*, *DECREASED APICAL DOMINANCE* (*DAD*) in *Petunia hybrida*, and *RAMOSUS* (*RMS*) in *Pisum sativum* were identified in which SLs act as endogenous signals [12, 14]. Many genes are involved in the biosynthesis of SLs, including *MAX3/RMS5/D17/DAD3*, *MAX4/RMS1/DAD1/D10*, and *OsMAX1/MAX1*. Some genes are components of the SL signaling pathway, such as *AtD27/D27*. *MAX2/D3/RMS4*, *D14/D88/HTD2*, *D53/SMAX1-LIKE*, and *BRC1/BRC2/FC1/OsTB1* [15-20]. *MAX2/RMS4/D3* genes are key factors that play vital roles in the SL signaling pathway [21, 22]. *MAX2*, in particular, functions at the intersection of multiple signaling pathways [23]. *MAX2* encodes an F-box leucine-rich repeat protein and constitutes part of a Skp-Cullin-F-box (SCF) E3 ligase complex, which functions downstream of *MAX3*, *MAX4*, and *MAX1* [24-26]. *MAX2* is involved in a series of functions that regulate plant developmental processes, senescence, karrikin signalin g, photomorphogenesis,

temperature signaling, SL signaling, drought response, and shoot architecture [10, 12, 21, 27-29]. In addition, *MAX2* functions at the signal intersection associated with SLs and other hormones, such as auxin, cytokinins, gibberellin, and jasmonates [21, 30-32]. SL-deficient *max* (*A. thaliana*), *rms* (*P. sativum*), *d* (*O. sativa*), and *dad* (*P. hybrida*) mutants have been studied widely owing to their enhanced shoot branching phenotype. The *max2* mutant has a relatively high tillering and dwarfing phenotype, and is insensitive to GR24, a synthetic SL analog [25, 33, 34]. It has been suggested that SLs inhibit auxin biosynthesis, which controls shoot branching and regulates plant root development [30, 35-37].

Tillering is critical for switchgrass productivity. In this study, we cloned the *PvMAX2* gene (the homolog of *AtMAX2*) from Alamo switchgrass and analyzed its biological characteristics. The Arabidopsis *max2* mutant has been transformed with *PvMAX2* to analyze the function of the gene. Overexpression of *PvMAX2* in the Arabidopsis *max2* mutant successfully complemented many phenotypes of the mutant, such as primary inflorescence length, branch number, and number of rosette leaves. In addition, we examined the response of wild type (WT), *max2*, and transgenic lines to GR24 and indole-3-acetic acid (IAA). Our results indicate that the overexpression of *PvMAX2* could almost completely complement the phenotype of the *max2* mutant, suggesting identification of the ortholog of *MAX2* in switchgrass.

2. Materials and methods

2.1 Plant materials and growth conditions

Arabidopsis ecotype Col-0 was used as the WT in this study. The *max2-1* mutant [24] was obtained from the Institute of Genetics and Developmental Biology (Beijing, China). Arabidopsis plants were grown in a chamber at 25°C with a 14-h light/10-h dark photoperiod and 70% humidity [38]. Before sowing on Murashige and Skoog (MS) plates, seeds were surface-sterilized with 70% (v/v) ethanol for 1 min and with 10% (w/v) sodium hypochlorite for 10 min, followed by three washes with sterile distilled

water. After stratification at 4°C for 3 days, the seeds were sown on half-strength MS medium containing 0.5% (w/v) sucrose and 0.75% (w/v) agar at pH 5.8 [39].

The Alamo switchgrass cultivar (autotetraploid, 2n = 4x = 36) was used for gene cloning and expression analysis. Switchgrass plants were propagated asexually by tiller-splitting and grown in the greenhouse at Northwest A & F University (Yangling, China) with a 16-h light/8-h dark photoperiod within a temperature range of 23–28°C.

2.2 *PvMAX2* gene cloning and vector construction

Based on the homologous sequence of *MAX2/D3/RMS4* in the switchgrass (Alamo) database (https://phytozome.jgi.doe.gov/pz/portal.html#!info?alias=Org_Pvirgatum_er), we designed switchgrass *MAX2* primers (*MAX2-F* and *MAX-R* in Table S1) to amplify the open reading frame (ORF) of the *PvMAX2* gene using Primer Premier 5.0 software. Using the Prime Script II 1st Strand cDNA Synthesis Kit (TaKaRa, Kusatsu, Japan), the template cDNA was synthesized from total RNA extracted from the shoots of the switchgrass lowland ecotype Alamo using the HiPure Plant RNA Mini Kit (Magen, Guangzhou, China) [40]. The polymerase chain reaction (PCR) product obtained by the KOD -Plus- high fidelity DNA polymerase (Toyobo, Ohtsu, Japan) was then cloned into the pGEM-T easy vector to be sequenced by Thermo Fisher Scientific Inc. (Shanghai, China).

The ORF of *PvMAX2* with *Bam*H1 and *Spe*1 restriction enzyme sites at the5’ and 3’ ends, respectively, obtained using primers *MAX2-Bam*H1 and *MAX2-Spe*1 (Table S1), was inserted into pTCK303 [41] to generate the construct for overexpression of *PvMAX2*, named *PvMAX2OE*.

2.3 Sequence and phylogenetic analysis

The ORF of the *PvMAX2* gene sequence was predicted using DNAMAN version 6.0 software, the physical and chemical properties of the encoded amino acid sequence were analyzed using ProtParam software. The F-box motif was identified by aligning the PvMAX2 sequence with those of other F-box proteins. A phylogenetic tree of

homologous proteins from dicot and monocot plants was constructed using MEGA 7 software by the neighbor-joining method [42, 43].

2.4 Arabidopsis transformation and *max2* mutant complementation

The *PvMAX2OE* construct was introduced into *Agrobacterium tumefaciens* (EHA105) to transform the Arabidopsis mutant *max2* using the floral-dip method [44]. Candidate transgenic plants were screened on half-strength MS medium containing 40 mg/L hygromycin B. The transgenic seedlings were identified using PCR with the Hyg primers (Table S1). We randomly selected at least 10 individual plants per homozygous line for phenotype observation. Three independent homozygous transgenic lines were used for further analysis.

Leaf area was measured using Image J software (NIH, USA) after seedlings had grown for 14 days following germination in soil. Rosette leaves were counted at the 22-day-old stage. We determined the number of branches and primary inflorescence length at the 50-day-old stage.

2.5 RNA extraction and quantitative real-time PCR (qRT-PCR)

Total RNA was extracted from transgenic Arabidopsis seedlings and switchgrass plant tissues (root, leaf, leaf sheath, shoot base, shoot node, and panicle) using the HiPure Plant RNA Mini Kit according to the manufacturer's instructions. The RNA sample was dissolved in 30 µL of diethylpyrocarbonate (DEPC)-treated water. Then, 1 µg of total RNA of each sample was reverse transcribed using the Prime Script RT reagent Kit with gDNA Eraser (Perfect Real Time; TaKaRa).

We performed qRT-PCR to determine gene expression. *PvActin* and *PvEF-1-alpha* were used as internal controls for switchgrass and *AtACTIN7* was used as an internal control for Arabidopsis. *PvMAX2* gene-specific primers (*PvMAX2Q-F* and *PvMAX2Q-R*) used in qRT-PCR are listed in Table S1. We performed qRT-PCR using the ABI 700 Real Time System (Applied Biosystems, USA) with SYBR Premix EX Taq II (Tli RNaseH plus) (TaKaRa). The reaction conditions were pre-incubation at 95°C for 5 s, followed by 40 cycles at 95°C for 30 s, 60°C for 31 s, and 72°C for 30 s.

The relative expression level in each sample was calculated using the $2^{-\Delta\Delta Ct}$ method [45].

2.6 GR24 and IAA treatment assay

Arabidopsis seeds were surface-sterilized, cooled at 4°C in the dark for three days, and then grown on half-strength MS plates. When the root length was ~1 cm, seedlings were gently transferred to half-strength MS plates containing various concentrations of GR24 or IAA. After seven days of vertical growth in an incubator, the primary root length was measured using Image J software. GR24 treatments were conducted at a concentration of 10^{-6} M, and 21 seedlings were measured for each genotype [46]. The IAA concentration was 10^{-7} M; 21 seedlings were measured from each line. Non-treated roots were used as the control in each experiment [47].

Switchgrass seeds were surface-sterilized and placed on wet filter paper. When the roots were 2 cm long, the seedlings were transferred to Hoagland nutrient solution renewed at 3-day intervals. Plants were grown in a 28°C incubator under 16-h light/8-h dark photoperiod conditions. After 20 days, samples were transferred separately to new cultures containing 10^{-5}, 10^{-6} and 10^{-7} M GR24 for 24 h before seedling collection for RNA extraction.

2.7 Hypocotyl elongation assay

To determine the hypocotyl length of each line, seeds were surface-sterilized, cooled at 4°C in the dark for 3 days and then plated on half-strength MS medium with various concentrations of GR24 or IAA. The seeds were exposed to white light for 3 h to encourage seedling photomorphogenesis at room temperature and then placed in a dark climate chamber at 25°C. After incubation in the dark for 5 days, the hypocotyl lengths of 20 individual seedlings from each line were then measured.

2.8 Statistical analyses

Most data were recorded from at least three independent experiments. Data are presented as means ± standard error of the mean [48]. Means were compared by

166 analysis of variance (ANOVA), followed by Duncan's multiple range test. Different
167 letters indicate significant differences between treatments ($P < 0.05$).

168 **3. Results**

169 **3.1 Cloning and sequence analysis of the *PvMAX2* gene**

170 To acquire the full length *PvMAX2* gene, we used protein sequences of AtMAX2
171 [24] and rice D3 [33] as queries to BLAST search the switchgrass (Alamo) database.
172 According to the database, 18 scaffolds named 01–09 (K or N) are ordered to match the
173 syntenic foxtail millet (*Setaria italica*) chromosome order. The results of the BLAST
174 search with AtMAX2 indicated three orthologs in the switchgrass genome:
175 *Pavir.4KG041800* (Chr04K:4096937.4099581) and *Pavir.4KG045300*
176 (Chr04K:4345003.4348920) on Chr. 4K and *Pavir.4NG045300*
177 (Chr04N:4630531.4632529) on Chr. 4N. The sequence of *Pavir.4KG041800* is the
178 same as that of *Pavir.4KG045300*. The sequence of *Pavir.4NG045300*, which is the
179 same as the latter part of *MAX2*, may be an incomplete *MAX2* sequence lacking the first
180 sequence region, because the first part of *MAX2* was found within sequences not
181 localized on chromosomes in the database (Fig. S1). There was a 37-bp gap between
182 *Pavir.4NG045300* and the unlocalized part compared with
183 *Pavir.4KG045300/P*avir.4KG041800. One PCR product of the switchgrass cDNA from
184 primers designed according to the preceding sequences possessed 6 bp less than
185 *Pavir.4NG045300/Pavir.4KG041800.* The product matched perfectly with
186 *Pavir.4NG045300* and the previous unlocalized sequence. Therefore, we conclude that
187 the switchgrass tetraploid genome likely contains two high-similarity *MAX2*
188 homologues, one of which is 6 bp longer than the other. We named the longest
189 homologue *PvMAX2* (GenBank accession number: MH172301); it contained 2,112 bp
190 with no introns and encoded a 703-amino acid protein.

191 Sequence analysis indicated that PvMAX2 contains an F-BOX motif at the
192 N-terminus (Fig. S2). Alignment with the MAX2 protein sequences from other species
193 showed that PvMAX2 had 92.60%, 87.29%, 76.67%, 41.39%, and 43.43% identities to

194 SiMAX2, SbMAX2, D3, RMS4, and AtMAX2, respectively (Fig. 1A). Phylogenetic
195 analysis of MAX2 homologs among switchgrass, Arabidopsis, pea, rice, millet, and
196 sorghum suggested that PvMAX2 is most closely related to millet SiMAX2, but
197 relatively less related to dicot Arabidopsis AtMAX2 and pea RMS4 (Fig. 1B).

198 **3.2 *PvMAX2* expression pattern in switchgrass**

199 According to the expression data in the Joint Genome Institute database,
200 *PvMAX2* is expressed in all tissues, with higher levels detected in the stem nodes and
201 roots (Fig. 2A). The homologs (*Pavir.4KG045300/Pavir.4KG041800*, and
202 *Pavir.4NG045300*) exhibited similar expression profile patterns. Expression levels of
203 *MAX2* were greatest in the roots in sorghum, and in the axillary buds and roots in
204 petunia [49, 50]. We detected *PvMAX2* expression by qRT-PCR in various tissues of
205 switchgrass including the stem base, leaf sheath, leaf, stem node, P1 panicle (early), and
206 P2 panicle (late). The highest levels were detected in the stem nodes, followed by the
207 stem base, root, leaf, and leaf sheath. The lowest expression levels were found in the P1
208 panicle (early) and P2 panicle (late) (Fig. 2B).

209 **3.3 *PvMAX2* expression in response to GR24 treatment**

210 As a key factor in the SL signal transduction pathway, the expression level of
211 *MAX2* is upregulated by GR24 [28, 51, 52]. In this study, the expression level of
212 *PvMAX2* was markedly increased in GR24-treated samples compared with the untreated
213 controls (Fig. 3).

214 **3.4 Ectopic expression of *PvMAX2* in the Arabidopsis *max2* mutant**

215 To confirm the functional orthology of *PvMAX2*, the *PvMAX2OE* construct was
216 introduced into the Arabidopsis *max2* mutant; 12 transgenic lines were successfully
217 obtained (Fig. S3B) and three lines were selected for subsequent trials. All three
218 transgenic lines had significantly higher expression levels of *PvMAX2* (Fig. 4B). The
219 shoots in the *max2* plants were shorter and had more lateral inflorescences than WT
220 plants [24, 25]. The transgenic *PvMAX2OE* plants displayed high branch lengths and
221 reduced tiller numbers. The transgenic plants L2, L3, and L4 partly rescued the bushy

phenotype and plant height to levels similar to those of WT plants. These results confirmed that the function of *PvMAX2* in branching regulation was similar to that of *AtMAX2* (Fig. 4A).

3.5 Complementation of the Arabidopsis *max2* mutant by *PvMAX2* at branching and leaf size

Compared with the *max2* mutant, the WT and three transgenic lines had visibly higher primary inflorescence lengths. The heights of the transgenic lines were 1.3 to 1.4 times that of the *max2* mutant but were shorter than the WT (Fig. 4C) which was 1.7 times that of the *max2* mutant. This result suggests that *PvMAX2* expression was not fully effective in conferring increased height in the Arabidopsis *max2* mutant. The WT and mutant plants had an average of 5.2 and 15.9 branches, respectively. The numbers of branches in the three *PvMAX2OE* transgenic lines in the *max2* mutant background were decreased markedly to the level of the WT (Fig. 4E). In addition, the numbers of rosette leaves in the transgenic lines were similar to that of the WT but reduced compared with the *max2* mutant (Fig. 4D). The *max2* mutant had smaller leaf blades at the early seedling stage than observed in WT [53]. Generally, *max2* mutant plants had smaller leaf blades than WT, and the leaves of the transgenic lines were restored to normal blade size in WT (Fig. 5). These results indicate that *PvMAX2* almost completely rescued the defect of the *max2* mutant during plant development and growth.

3.6 Effects of GR24 and IAA on primary root length

Previous studies demonstrated that SLs were involved in root phenotypes in a MAX2-dependent manner [47]. GR24 inhibited root development at relatively high concentrations and promoted primary root length at low concentrations [39, 54]. To determine whether *PvMAX2* could complement the root growth phenotype of the *max2* mutant, we measured the primary root lengths of all lines. The *max2* mutant had shorter primary root lengths than the WT and *PvMAX2OE* transgenic plants. In addition, the primary root of *max2* showed no response to GR24 treatment, while the response to

GR24 was restored in the transgenic plants to levels similar to WT (Fig. 6A). IAA could reduce the length of WT primary roots within a certain concentration range, and auxin interacted with SLs in the regulation of primary root development [54-56]. We found that the response to IAA treatment was similar among the mutant, WT, and *PvMAX2OE* transgenic lines; IAA inhibited root growth regardless of the normal function of MAX2 (Fig. 6B).

3.7 Effects of GR24 and IAA on hypocotyl elongation

The *max2* mutant displayed a longer hypocotyl than WT in light-grown seedlings, but similar hypocotyl length to that of WT when grown in the dark [21, 24, 52]. Previous studies reported that IAA could inhibit hypocotyl growth at any concentration [57]. We investigated the effect of GR24 and auxin on hypocotyl elongation by measuring hypocotyl lengths in seedlings of WT, *max2*, and *PvMAX2OE* transgenic lines. The hypocotyl length of *max2* seedlings was markedly higher than that in seedlings of the WT and the three transgenic lines. The hypocotyl length of *max2* was insensitive to GR24, whereas the hypocotyl length was reduced slightly in GR24-treated WT and transgenic lines (Fig. 7A). These results indicate that hypocotyl elongation is inhibited by GR24 in the presence of normal *MAX2* function under dark growth conditions. However, regardless of the presence or absence of normal MAX2 function, the hypocotyl lengths were reduced dramatically by IAA treatment (Fig. 7B). These results indicate that *PvMAX2* can substitute for *AtMAX2* in regulating hypocotyl development in the dark.

4. Discussion

Switchgrass, a perennial energy crop in the USA, has received heightened research attention due to its high energy conversion efficiency from biomass to fuel alcohol [3, 58-60]. Recent studies have focused on branching/tillering to improve the biomass of switchgrass [61]. Previous studies revealed that *MAX2/D3/RMS4* genes regulate plant architecture, senescence, karrikin signaling, temperature responses, and photomorphogenesis [17, 21, 24, 62, 63]. However, it is unclear whether such

278 regulation occurs in switchgrass. Therefore, we investigated the role of the SL signal
279 transduction factor *MAX2* in switchgrass.

280 In this study, we identified an ortholog of *MAX2* (*PvMAX2*) in switchgrass; it
281 encodes an F-box protein that is closest to SiMAX2 in foxtail millet (*Setaria italica*)
282 (Fig. 1B). When *PvMAX2* was expressed in the Arabidopsis *max2* mutant, most
283 phenotypes of the *max2* mutant were rescued. However, due to the different insertion
284 site of *PvMAX2* on the Arabidopsis genome or functional differentiation among
285 different species, the ectopic expression of the *PvMAX2* cannot entirely complement the
286 *AtMAX2*. SLs are widely recognized as shoot branching regulators; the *max2* mutant
287 produces increased branch numbers. Previous studies have shown that branching in the
288 Arabidopsis *max2* mutant was restored to the normal level after transformation with the
289 *ShMAX2* gene, isolated from the parasite *Striga hermonthica* [28]. The branching
290 phenotype of the Arabidopsis *max2* mutant is also almost fully complemented by
291 *DgMAX2a* [64]. Our results indicated that the expression of *PvMAX2* in the Arabidopsis
292 *max2* mutant partially rescued the inflorescence length and branch number mutant
293 phenotypes (Fig. 4A, 4C, and 4E). Other studies of *MAX2* in different species revealed
294 that *OaMAX2* and *GmMAX2a*, the ortholog of the Arabidopsis *MAX2* gene in soybean
295 and *Orobanche aegyptiaca*, were able to rescue the leaf size of the Arabidopsis *max2*
296 mutant [32, 53]. We also observed that *PvMAX2* expression almost restored leaf
297 phenotypes in the early developmental stages (Fig. 5). Together, these results indicate
298 the complementary effects of *PvMAX2* for loss-of-function of *AtMAX2* in both the early
299 and late developmental stages. This partial rescue may be caused by the functional
300 differences between *PvMAX2* and *AtMAX2*, which may be due to functional
301 differentiation between monocot and dicot species.

302 Our results revealed that GR24 enhanced primary root length at a concentration
303 of 10^{-6} M, while the *max2* mutant was insensitive to GR24 (Fig. 6A). The *max2* mutant
304 had a shorter root, possibly due to the reduction in cell number in the primary root
305 meristem [65]. In support of our results, the *OaMAX2* gene from the parasitic *O.*

306 *aegyptiaca* could also complement the shorter primary root length of *max2* [53].
307 Previous studies have reported that the primary root length of *max2* decreased under
308 high-concentration GR24 treatments due to general toxicity, and the other phenotype of
309 *max2* could not be rescued by application of GR24 [39]. *MAX2* was shown to be
310 involved in photomorphogenesis. WT and *max2* seedlings have similar hypocotyl
311 lengths in the dark. However, hypocotyl elongation was inhibited by SLs in WT,
312 whereas hypocotyl elongation was unaffected by GR24 treatment in the *max2* mutant
313 [21, 28, 52, 66]. We found that the *max2* seedlings exhibited markedly longer hypocotyl
314 length than the WT, and the ectopic expression of *PvMAX2* in *max2* reduced the
315 hypocotyl length (Fig. 7A). These results suggest that many factors likely affect
316 hypocotyl elongation. A recent study showed that SLs inhibited hypocotyl elongation
317 depending on cryptochrome and phytochrome signaling, and that high doses of GR24
318 inhibited hypocotyl elongation in both light and dark conditions [67]. These results
319 indicate that GR24 inhibits hypocotyl growth below a GR24 concentration threshold.
320 Moreover, *MAX2* is necessary for the hypocotyl elongation responses to SLs.
321 Previous studies show that auxin transport is necessary for the branching phenotype of
322 the *max2* mutants. There are multiple interactions at different levels between SLs and
323 auxin [30, 35, 38]. IAA can reduce the length of the WT primary root below a certain
324 concentration of GR24 [55]. IAA has been suggested to be involved in SLs, affecting
325 root development and decreasing primary root length by reducing cell length [54, 56].
326 Recently, it was reported that *MdMAX2* regulated hypocotyl elongation, particularly by
327 influencing auxin transport in apple [68]. These results indicate that auxin interacts with
328 SLs to regulate root and hypocotyl development. However, the interactions between SLs
329 and auxin may be quite complex [67, 69]. Our studies showed that the primary root and
330 hypocotyl lengths decreased dramatically following IAA treatment in WT, the *max2*
331 mutant, and the *PvMAX2OE* transgenic lines in the *max2* background (Figs. 6B, 7B).
332 These results indicate that *PvMAX2* acts upstream of auxin in root and hypocotyl
333 development.

5. Conclusion

The findings of our study suggest that *PvMAX2* has a conserved function in regulating plant shoot branching. The *PvMAX2* gene we identified in switchgrass not only inhibited shoot branching but also rescued the *max2* mutant phenotype in roots. These findings provide a theoretical foundation for the utilization of *PvMAX2* in switchgrass. In addition, we revealed that *AtMAX2* and *PvMAX2* exhibit slight differences in function and may regulate plant development through different regulatory networks that may correspond to differences between monocots and dicots. The function of *PvMAX2* in switchgrass requires further research.

Contributions

Tingting Cheng and Fengli Sun conceived and designed the study. Tingting Cheng, Donghua Wang, Yongfeng Wang, and Shumeng Zhang performed the experiments. Tingting Cheng wrote the paper. Fengli Sun, Chao Zhang, Shudong Liu, and Yajun Xi reviewed and edited the manuscript. All authors read and approved the manuscript.

Acknowledgments:

We thank Jiayang Li (Institute of Genetics and Developmental Biology, Beijing, China) for providing the *max2-1* mutant seeds. This project was supported by the National Natural Science Foundation of China (NO. 31301384, 31371690, 31601370).

Conflicts of Interest

The authors have no conflicts of interest to declare.

References

[1] I. Lewandowski, J.M.O. Scurlock, E. Lindvall, M. Christou, The development and current status of perennial rhizomatous grasses as energy crops in the US and Europe, Biomass and Bioenergy, 25 (2003) 335-361.

[2] S. B. McLaughlin, L. Adams Kszos, Development of switchgrass (*Panicum virgatum*) as a bioenergy feedstock in the United States, Biomass and Bioenergy, 28 (2005) 515-535.

[3] M.R. Schmer, K.P. Vogel, R.B. Mitchell, R.K. Perrin, Net energy of cellulosic ethanol from switchgrass, Proceedings of the National Academy of Sciences of the United States of America, 105 (2008) 464-469.

[4] G.K. Evanylo, A.O. Abaye, C. Dundas, C.E. Zipper, R. Lemus, B. Sukkariyah, J. Rockett, Herbaceous vegetation productivity, persistence, and metals uptake on a biosolids-amended mine soil, Journal of Environmental Quality, 34 (2005) 1811-1819.

[5] M.A. Sanderson, R.L. Reed, S.B. McLaughlin, S.D. Wullschleger, B.V. Conger, D.J. Parrish, D.D. Wolf, C. Taliaferro, A.A. Hopkins, W.R. Ocumpaug, Switchgrass as a sustainable bioenergy crop, Bioresource Technology, 56 (1996) 83-93.

[6] J,B. Evers, A,R. van der Krol, J. Vos1, P.C. Struik, Understanding shoot branching by modelling form and function, Trends in Plant Science, 16 (2011) 464-467.

[7] C.A. Beveridge, J.L. Weller, S.R. Singer, J.M. Hofer, Axillary meristem development. Budding relationships between networks controlling flowering, branching, and photoperiod responsiveness, Plant Physiology, 131 (2003) 927-934.

[8] T.H. Kebrom, W. Spielmeyer, E.J. Finnegan, Grasses provide new insights into regulation of shoot branching, Trends in Plant Science, 18 (2013) 41-48.

[9] H. Klee, Plant biology - Hormones branch out, Nature, 455 (2008) 176-177.

[10] V. Gomez-Roldan, S. Fermas, P.B. Brewer, V. Puech-Pages, E.A. Dun, J.P. Pillot, F. Letisse, R. Matusova, S. Danoun, J.C. Portais, H. Bouwmeester, G. Becard, C.A. Beveridge, C. Rameau, S.F. Rochange, Strigolactone inhibition of shoot branching, Nature, 455 (2008) 189-194.

[11] M. Umehara, A. Hanada, S. Yoshida, K. Akiyama, T. Arite, N. Takeda-Kamiya, H. Magome, Y. Kamiya, K. Shirasu, K. Yoneyama, J. Kyozuka, S. Yamaguchi, Inhibition of shoot branching by new terpenoid plant hormones, Nature, 455 (2008) 195-200.

[12] S. Al-Babili, H.J. Bouwmeester, Strigolactones, a novel carotenoid-derived plant hormone, Annual Review of Plant Biology, 66 (2015) 161-186.

[13] C.E. Cook, L.P. Whichard, B. Turner, M.E. Wall, G.H. Egley, Germination of witchweed (*Striga lutea* Lour.): Isolation and properties of a potent stimulant, Science (New York, N.Y.), 154 (1966) 1189-1190.

[14] A. de Saint Germain, S. Bonhomme, F.D. Boyer, C. Rameau, Novel insights into strigolactone distribution and signalling, Current Opinion in Plant Biology, 16 (2013) 583-589.

[15] H. Lin, R. Wang, Q. Qian, M. Yan, X. Meng, Z. Fu, C. Yan, B. Jiang, Z. Su, J. Li, Y. Wang, DWARF27, an iron-containing protein required for the biosynthesis of strigolactones, regulates rice tiller bud outgrowth, The Plant Cell, 21 (2009) 1512-1525.

[16] T. Waldie, H. McCulloch, O. Leyser, Strigolactones and the control of plant development: lessons from shoot branching, The Plant Journal, 79 (2014) 607-622.

[17] M.T. Waters, D.C. Nelson, A. Scaffidi, G.R. Flematti, Y.K. Sun, K.W. Dixon, S.M. Smith, Specialisation within the DWARF14 protein family confers distinct responses to karrikins and strigolactones in Arabidopsis, Development, 139 (2012) 1285-1295.

[18] K. Minakuchi, H. Kameoka, N. Yasuno, M. Umehara, L. Luo, K. Kobayashi, A. Hanada, K. Ueno, T. Asami, S. Yamaguchi, J. Kyozuka, FINE CULM1 (FC1) works downstream of strigolactones to inhibit the outgrowth of axillary buds in rice, Plant & Cell Physiology, 51 (2010) 1127-1135.

[19] F. Zhou, Q. Lin, L. Zhu, Y. Ren, K. Zhou, N. Shabek, F. Wu, H. Mao, W. Dong, L. Gan, W. Ma, H. Gao, J. Chen, C. Yang, D. Wang, J. Tan, X. Zhang, X. Guo, J. Wang, L. Jiang, X. Liu, W. Chen, J. Chu, C. Yan, K. Ueno, S. Ito, T. Asami, Z. Cheng, J. Wang, C. Lei, H. Zhai, C. Wu, H. Wang, N. Zheng, J. Wan, D14-SCF(D3)-dependent degradation of D53 regulates strigolactone signalling, Nature, 504 (2013) 406-410.

[20] J.A. Aguilar-Martinez, C. Poza-Carrion, P. Cubas, Arabidopsis BRANCHED1 acts as an integrator of branching signals within axillary buds, The Plant Cell, 19 (2007) 458-472.

[21] H. Shen, L. Zhu, Q.-Y. Bu, E. Huq, MAX2 affects multiple hormones to promote photomorphogenesis, Molecular Plant, 5 (2012) 750-762.

[22] M. Marzec, Perception and signaling of strigolactones, Frontiers in Plant Science, 7 (2016) 1260.

[23] N. Morffy, L. Faure, D.C. Nelson, Smoke and hormone mirrors: action and evolution of karrikin and strigolactone signaling, Trends in Genetics, 32 (2016).

[24] P. Stirnberg, K. van De Sande, H.M. Leyser, MAX1 and MAX2 control shoot lateral branching in Arabidopsis, Development, 129 (2002) 1131-1141.

[25] P. Stirnberg, I.J. Furner, H.M. Ottoline Leyser, MAX2 participates in an SCF complex which acts locally at the node to suppress shoot branching, The Plant Journal, 50 (2007) 80-94.

[26] X. Johnson, T. Brcich, E.A. Dun, M. Goussot, K. Haurogne, C.A. Beveridge, C. Rameau, Branching genes are conserved across species. Genes controlling a novel signal in pea are coregulated by other long-distance signals, Plant Physiology, 142 (2006) 1014-1026.

[27] H. Shen, P. Luong, E. Huq, The F-box protein MAX2 functions as a positive regulator of photomorphogenesis in Arabidopsis, Plant Physiology, 145 (2007) 1471-1483.

[28] Q. Liu, Y. Zhang, R. Matusova, T. Charnikhova, M. Amini, M. Jamil, M. Fernandez-Aparicio, K. Huang, M.P. Timko, J.H. Westwood, C. Ruyter-Spira, S. van der Krol, H.J. Bouwmeester, Striga hermonthica MAX2 restores branching but not the Very Low Fluence Response in the Arabidopsis thaliana max2 mutant, The New Phytologist, 202 (2014) 531-541.

441 [29] Q. Bu, T. Lv, H. Shen, P. Luong, J. Wang, Z. Wang, Z. Huang, L. Xiao, C. Engineer,
442 T.H. Kim, J.I. Schroeder, E. Huq, Regulation of drought tolerance by the F-box
443 protein MAX2 in Arabidopsis, Plant Physiology, 164 (2014) 424-439.
444 [30] P. Stirnberg, S. Ward, O. Leyser, Auxin and strigolactones in shoot branching:
445 intimately connected?, Biochemical Society Transactions, 38 (2010) 717-722.
446 [31] M. Tanaka, K. Takei, M. Kojima, H. Sakakibara, H. Mori, Auxin controls local
447 cytokinin biosynthesis in the nodal stem in apical dominance, The Plant Journal, 45
448 (2006) 1028-1036.
449 [32] B.U. Haq, M.Z. Ahmad, N. Ur Rehman, J. Wang, P. Li, D. Li, J. Zhao, Functional
450 characterization of soybean strigolactone biosynthesis and signaling genes in
451 Arabidopsis MAX mutants and GmMAX3 in soybean nodulation, BMC Plant
452 Biology, 17 (2017) 259.
453 [33] S. Ishikawa, M. Maekawa, T. Arite, K. Onishi, I. Takamure, J. Kyozuka,
454 Suppression of tiller bud activity in tillering dwarf mutants of rice, Plant & Cell
455 Physiology, 46 (2005) 79-86.
456 [34] Y. Tsuchiya, P. McCourt, Strigolactones: a new hormone with a past, Current
457 Opinion in Plant Biology, 12 (2009) 556-561.
458 [35] S. Saini, I. Sharma, N. Kaur, P.K. Pati, Auxin: a master regulator in plant root
459 development, Plant Cell Reports, 32 (2013) 741-757.
460 [36] D. Muller, O. Leyser, Auxin, cytokinin and the control of shoot branching, Annals of
461 Botany, 107 (2011) 1203-1212.
462 [37] D. Sang, D. Chen, G. Liu, Y. Liang, L. Huang, J.C. X Meng, X. Sun, G. Dong, Y.
463 Yuan, Q. Qian, J. Li, Y. Wang, Strigolactones regulate rice tiller angle by attenuating
464 shoot gravitropism through inhibiting auxin biosynthesis, Proceedings of the
465 National Academy of Sciences of the United States of America, 111 (2014)
466 11199–11204.

[38] T. Bennett, T. Sieberer, B. Willett, J. Booker, C. Luschnig, O. Leyser, The Arabidopsis MAX pathway controls shoot branching by regulating auxin transport, Current Biology, 16 (2006) 553-563.

[39] C. Ruyter-Spira, W. Kohlen, T. Charnikhova, A. van Zeijl, L. van Bezouwen, N. de Ruijter, C. Cardoso, J.A. Lopez-Raez, R. Matusova, R. Bours, F. Verstappen, H. Bouwmeester, Physiological effects of the synthetic strigolactone analog GR24 on root system architecture in Arabidopsis: another belowground role for strigolactones?, Plant Physiol, 155 (2011) 721-734.

[40] K. J. Moore, L.E. Mosser, K. P. Vogel, S. S. Waller, B. E. Johnson, J.F. Pederson. Describing and quantifying growth stages of perennial forage grasses, Agronomy Journal, 83 (1991) 1073-1077.

[41] Z. Wang, C. Chen, Y. Xu, R. Jiang, Y. Han, Z. Xu, K. Chong, A practical vector for efficient knockdown of gene expression in rice (*Oryza sativa* L.), Plant Molecular Biology Reporter, 22 (2004) 409-417.

[42] K. Tamura, D. Peterson, N. Peterson, G. Stecher, M. Nei, S. Kumar, MEGA5: molecular evolutionary genetics analysis using maximum likelihood, evolutionary distance, and maximum parsimony methods, Molecular Biology and Evolution, 28 (2011) 2731-2739.

[43] N. Saitou, M. Nei, The neighbor-joining method: A new method for reconstructing phylogenetic trees, Molecular Biology and Evolution, 4 (1987) 406-425.

[44] S.J. Clough, A.F. Bent, Floral dip: a simplified method for Agrobacterium-mediated transformation of *Arabidopsis thaliana*, The Plant Journal 16 (1998) 735–743.

[45] K.J. Livak, T.D. Schmittgen, Analysis of relative gene expression data using real-time quantitative PCR and the $2^{-\Delta\Delta CT}$ method, Methods, 25 (2001) 402-408.

[46] L.J. Bromhead, J. Visser, C.S. McErlean, Enantioselective synthesis of the strigolactone mimic (+)-GR24, The Journal of Organic Chemistry, 79 (2014) 1516-1520.

494 [47] Y. Kapulnik, P.M. Delaux, N. Resnick, E. Mayzlish-Gati, S. Wininger, C.
495 Bhattacharya, N. Sejalon-Delmas, J.P. Combier, G. Becard, E. Belausov, T.
496 Beeckman, E. Dor, J. Hershenhorn, H. Koltai, Strigolactones affect lateral root
497 formation and root-hair elongation in Arabidopsis, Planta, 233 (2011) 209-216.
498 [48] S. Maríaj, F. Mónica, C.M. Vilma, G. Josém, O. Juana, D. Maríaj, V. Horst, First
499 indications for the involvement of strigolactones on nodule formation in alfalfa
500 (*Medicago sativa*), Soil Biology & Biochemistry, 42 (2010) 383-385.
501 [49] T.H. Kebrom, T.P. Brutnell, S.A. Finlayson, Suppression of sorghum axillary bud
502 outgrowth by shade, phyB and defoliation signalling pathways, Plant, Cell &
503 Environment, 33 (2010) 48-58.
504 [50] R.S. Drummond, H. Sheehan, J.L. Simons, N.M. Martinez-Sanchez, R.M. Turner, J.
505 Putterill, K.C. Snowden, The expression of petunia strigolactone pathway genes is
506 altered as part of the endogenous developmental program, Frontiers in Plant
507 Science, 2 (2011) 115.
508 [51] S. Li, L. Chen, Y. Li, R. Yao, F. Wang, M. Yang, M. Gu, F. Nan, D. Xie, J. Yan,
509 Effect of GR24 stereoisomers on plant development in Arabidopsis, Molecular
510 Plant, 9 (2016) 1432-1435.
511 [52] Y. Tsuchiya, D. Vidaurre, S. Toh, A. Hanada, E. Nambara, Y. Kamiya, S. Yamaguchi,
512 P. McCourt, A small-molecule screen identifies new functions for the plant hormone
513 strigolactone, Nature Chemical Biology, 6 (2010) 741-749.
514 [53] W. Li, K.H. Nguyen, Y. Watanabe, S. Yamaguchi, L.S. Tran, OaMAX2 of
515 *Orobanche aegyptiaca* and Arabidopsis AtMAX2 share conserved functions in both
516 development and drought responses, Biochemical and Biophysical Research
517 Communications, 478 (2016) 521-526.
518 [54] H. Koltai, E. Dor, J. Hershenhorn, D.M. Joel, S. Weininger, S. Lekalla, H. Shealtiel,
519 C. Bhattacharya, E. Eliahu, N. Resnick, R. Barg, Y. Kapulnik, Strigolactones' effect
520 on root growth and root-hair elongation may be mediated by auxin-efflux carriers,
521 Journal of Plant Growth Regulation, 29 (2010) 129-136.

[55] L. Hobbie, M. Estelle, The axr4 auxin-resistant mutants of Arabidopsis thaliana define a gene important for root gravitropism and lateral root initiation, The Plant Journal 7(1995) 211-220.

[56] X. Cheng, C. Ruyter-Spira, H. Bouwmeester, The interaction between strigolactones and other plant hormones in the regulation of plant development, Frontiers in Plant Science, 4 (2013) 199-199.

[57] C.E. Collett, N.P. Harberd, O. Leyser, Hormonal interactions in the control of Arabidopsis hypocotyl elongation, Plant Physiology, 124 (2000) 553-561.

[58] M.A. Sanderson, P.R. Adler, A.A. Boateng, M.D. Casler, A.G. Sarath, Switchgrass as a biofuels feedstock in the USA, Canadian Journal of Plant Science, 86 (2006) 1315-1325.

[59] D.J. Parrish, M.D. Casler, A. Monti, The evolution of switchgrass as an energy crop, Green Energy and Technology, (2012) 1-28.

[60] C.O. Hong, V.N. Owens, D. Bransby, R. Farris, J. Fike, E. Heaton, S. Kim, H. Mayton, R. Mitchell, D. Viands, Switchgrass response to nitrogen fertilizer across diverse environments in the USA: a regional feedstock partnership report, Bioenergy Research, 7 (2014) 777-788.

[61] Y. Wang, X. Zeng, L. Peal, Y. Tang, Y. Wu, R. Mahalingam, Transcriptome analysis of nodes and buds from high and low tillering switchgrass inbred lines, PLOS ONE, 8 (2013).

[62] H.R. Woo, K.M. Chung, J.-H. Park, S.A. Oh, T. Ahn, S.H. Hong, S.K. Jang, H.G. Nam, ORE9, an F-box protein that regulates leaf senescence in Arabidopsis, The Plant Cell, 13 (2001) 1779–1790.

[63] D.C. Nelson, J.A. Riseborough, G.R. Flematti, J. Stevens, E.L. Ghisalberti, K.W. Dixon, S.M. Smith, Karrikins discovered in smoke trigger Arabidopsis seed germination by a mechanism requiring gibberellic acid synthesis and light, Plant Physiology, 149 (2009) 863-873.

549 [64] L. Dong, A. Ishak, J. Yu, R. Zhao, L. Zhao, Identification and functional analysis of
550 three MAX2 orthologs in chrysanthemum, Journal of Integrated Plant Biology, 55
551 (2013) 434-442.
552 [65] H. Koltai, Strigolactones are regulators of root development, New Phytologist, 190
553 (2011) 545-549.
554 [66] D.C. Nelson, A. Scaffidi, E.A. Dun, M.T. Waters, G.R. Flematti, K.W. Dixon, C.A.
555 Beveridge, E.L. Ghisalberti, S.M. Smith, F-box protein MAX2 has dual roles in
556 karrikin and strigolactone signaling in *Arabidopsis thaliana*, Proceedings of the
557 National Academy of Sciences of the United States of America, 108 (2011)
558 8897-8902.
559 [67] K.P. Jia, Q. Luo, S.B. He, X.D. Lu, H.Q. Yang, Strigolactone-regulated hypocotyl
560 elongation is dependent on cryptochrome and phytochrome signaling pathways in
561 Arabidopsis, Molecular Plant, 7 (2014) 528-540.
562 [68] J.P. An, R. Li, F.J. Qu, C.X. You, X.F. Wang, Y.J. Hao, Apple F-box protein
563 MdMAX2 regulates plant photomorphogenesis and stress response, Frontiers of
564 Plant Science, 7 (2016) 1685.
565 [69] H. Sun, J. Tao, M. Hou, S. Huang, S. Chen, Z. Liang, T. Xie, Y. Wei, X. Xie, K.
566 Yoneyama, G. Xu, Y. Zhang, A strigolactone signal is required for adventitious root
567 formation in rice, Annals of Botany, 115 (2015) 1155-1162.
568

569 **Figure legends**

570 Fig. 1 Sequence alignment and phylogenetic analyses of MAX2 proteins.
571 A. Alignment of the PvMAX2 protein sequence with the Arabidopsis MAX2, pea
572 RMS4, and rice D3 protein sequences. Amino acids highlighted in orange, pink, and
573 blue represent residues that are completely conserved, partially conserved, and similar
574 to the consensus sequence, respectively. The alignment was generated using the
575 MegAlign and ClustalW programs (http://www.genome.jp/tools-bin/clustalw).

576 B. Phylogenetic tree analysis of MAX2 homologs from various species. A
577 neighbor-joining tree (Jones-Taylor-Thornton model) was generated using MEGA7 with
578 1000 replicates to generate bootstrap values. Species included were: Arabidopsis
579 (*Arabidopsis thaliana*), *AtMAX2* (NP_565979.1); *Sorghum bicolor*, *SbMAX2*
580 (XP_002436499.1); foxtail millet (*Setaria italica*), *SiMAX2* (XP_004964817.1); rice
581 (*Oryza sativa*), *OsD3* (NP_001174608.1); and pea (*Pisum sativum*), *RMS4*
582 (ABD67495.1).
583
584 Fig. 2 *MAX2* expression in various switchgrass tissues and *PvMAX2* gene expression
585 pattern. A, *MAX2* expression patterns in various switchgrass tissues. The expression
586 level of homologous genes Pavir.4KG045300/Pavir.4KG041800 (orange color) and
587 Pavir.4NG045300 (blue color) (retrieved from https://phytozome.jgi.doe.gov/pz/
588 portal.html#!search?show=BLAST). The expression profile was generated using
589 HemI1.0.3.3 software. B, *PvMAX2* expression pattern determined by qRT-PCR. R, root;
590 S, shoot base; L, leaf; SH, leaf sheath; SN, shoot node; P1, panicle (early); P2, panicle
591 (late); reference gene: *PvActin*. Leaf, leaf sheath, stem node, and P1 ear were collected
592 at the early heading stage, and the P2 ear was collected in the later heading stage. Roots
593 were collected from developing seedlings grown hydroponically. Error bars indicate the
594 standard deviation (SD).
595
596 Fig. 3 *PvMAX2* expression in switchgrass in response to GR24 treatment.
597 *PvMAX2* gene response to GR24. The tillers of 19-day-old plants grown in the absence
598 and presence of GR24 treatment for 24 h in hydroponics were collected and used for
599 RNA extraction. A 0.001% concentration of acetone without any GR24 was used as a
600 control. The reference gene was *PvEF-1-alpha*. Error bars indicate the standard
601 deviation (SD).
602

Fig. 4 *PvMAX2* expression levels and Arabidopsis *max2* branching phenotype with ectopic *PvMAX2* expression. A. Comparison of phenotypes of Col-0 wild type (WT), *max2-1*, and transgenic lines after 35 days of growth (left to right: WT, *max2*, L2, L3, L4). Bar = 5 cm. B. Quantitative real time (qRT)-PCR analysis of *PvMAX2* expression in transgenic lines (L2–L4). The reference gene was *AtActin7*. C. Primary inflorescence length in WT, *max2*, and three transgenic lines (L2–L4). Plants were analyzed near maturity, the primary inflorescence had ceased growing (after 50 days of growth). D. Number of rosette leaves in WT, *max2*, and three transgenic lines (L2–L4). Rosette leaves data were collected near the bolting stage (after 22 days of growth). E. Number of branches in WT, *max2*, and three transgenic lines (L2–L4). Branches with a length of at least 2 cm were counted. Values are the mean ± standard error of the mean (SEM; n = 10) from three independent experiments. Letters denote statistically significant differences between means at $P < 0.05$, according to one-way analysis of variance (ANOVA), followed by Duncan's multiple range test.

Fig. 5 Arabidopsis *max2* leaf phenotype with ectopic *PvMAX2* expression. A. Plants were photographed at the 2-week-old seedling stage. B. Leaf areas of the largest rosette leaves from WT, *max2*, and three transgenic lines (L2–L4). Values are the mean ± SEM (n = 15). Letters denote statistically significant differences between means at $P < 0.05$ (ANOVA). Bar = 0.2 cm.

Fig. 6 Phenotypes of WT, *max2*, and three transgenic lines (L2–L4) under various GR24 and indole-3-acetic acid (IAA) conditions. A. Primary root length of WT, *max2*, and three transgenic lines (L2–L4) treated with GR24. B. Primary root length of WT, *max2*, and three transgenic lines (L2–L4) treated with IAA. Data were collected after 7 days of growth in an incubator at 25°C with a 14-h light/10-h dark photoperiod. Values are the mean ± SEM (n = 21). Letters denote statistically significant differences between means at $P < 0.05$ (ANOVA).

Fig. 7 Complementation of Arabidopsis *max2* hypocotyl phenotypes. A. Assays of hypocotyl length sensitivity to GR24 in 5-day-old seedlings of WT, *max2*, and three transgenic lines (L2–L4) grown in the dark. B. Assays of hypocotyl length sensitivity to IAA in 5-day-old seedlings of WT, *max2*, and three transgenic lines (L2–L4) grown in the dark. Values are the mean ± SEM (n > 21). Letters denote statistically significant differences between means at $P < 0.05$ (ANOVA).

Fig. S1 Alignment of the nucleotide sequences of *Pavir.4KG045300*, *Pavir.4NG045300*, and *PvMAX2*.
The red box in the photo shows the gap between the unlocalized part and *Pavir.4NG045300*.

Fig. S2 Analysis of the amino acid sequence of *PvMAX2* from switchgrass. The F-box domain is underlined in red.

Fig. S3 A. Construction of the *PvMAX2* overexpression vector. The lengths of the *PvMAX2* gene (2,112 bp) and T-easy vector (white). The *PvMAX2*–pTCK303 fusion plasmid (left, white), Marker: 2,000-bp DNA molecular markers.
B. Transgenic Arabidopsis plant identification. PCR analysis of DNA samples from regenerated plants using primer specific for the hygromycin resistance gene. 1, negative control; 2, positive control (*PvMAX2–pTCK303* plasmid); 3–15, transgenic lines. Marker: 2,000-bp DNA molecular markers.

A

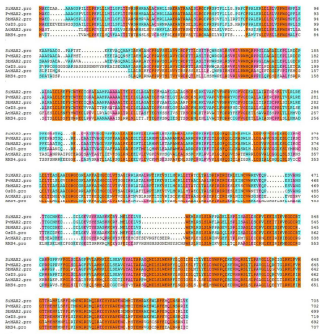

B

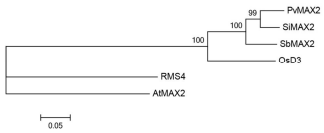

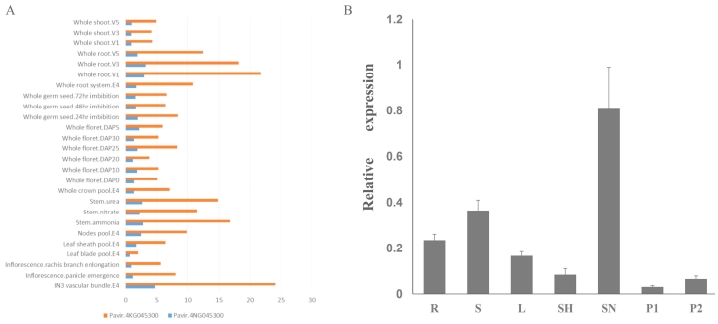

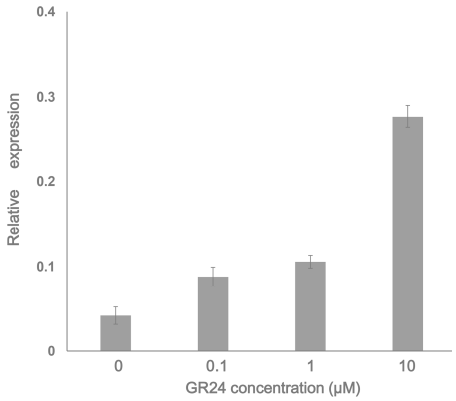

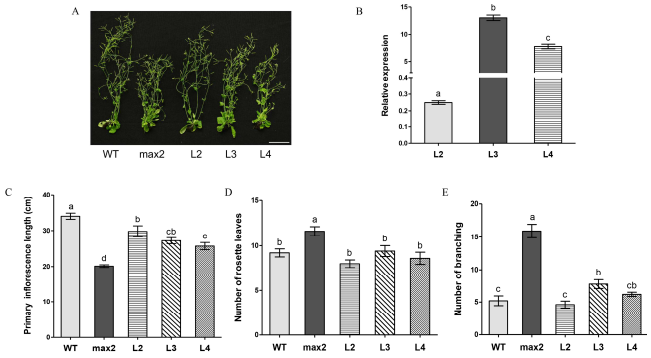

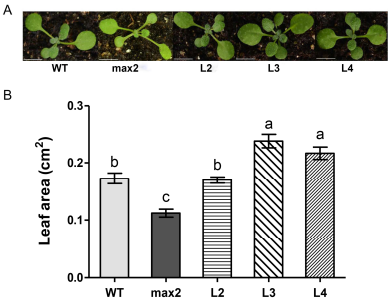

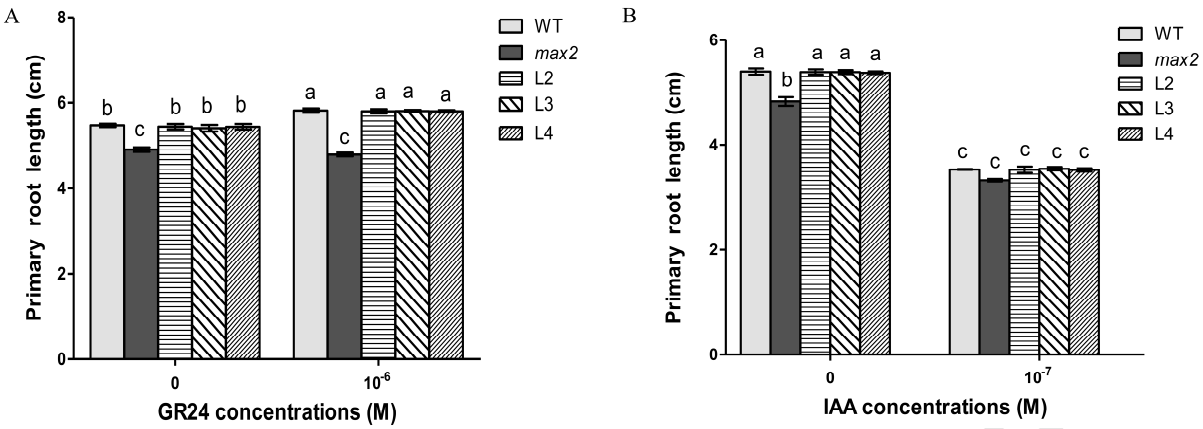

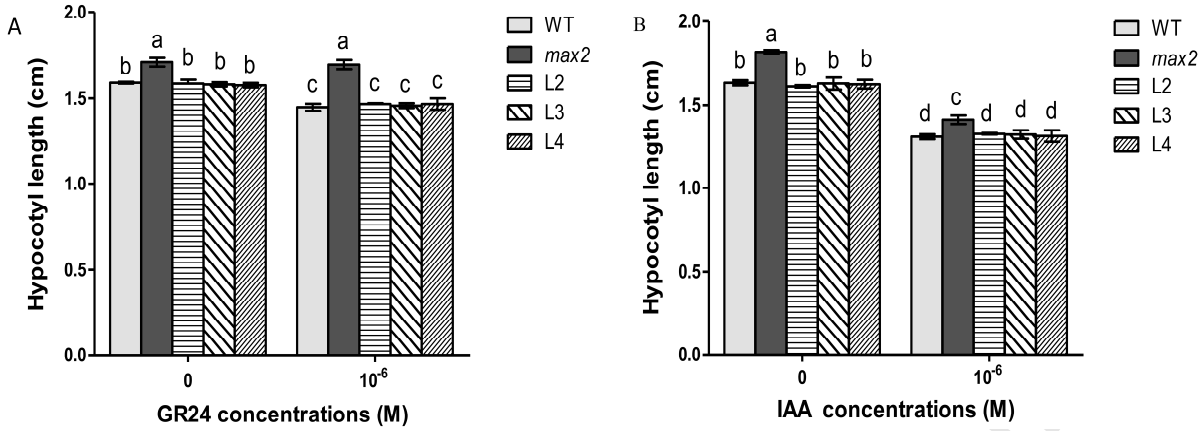

1. The gene *PvMAX2*, ortholog of *AtMAX2*, was identified in switchgrass.
2. *PvMAX2* was expressed at high level in shoot node, shoot base and root of switchgrass.
3. The overexpression of *PvMAX2* rescued the phenotype of Arabidopsis *max2* mutant.